Site Discrimination and Anisotropic Growth Inhibition by Molecular Imposters on Highly Dissymmetric Crystal Surfaces

*Laura N. Poloni,[†] Anthony P. Ford,[#] and Michael D. Ward[†,]**

[#]*Afferent Pharmaceuticals, 2929 Campus Dr., Suite 230, San Mateo, CA 94403, USA*

[†]*Department of Chemistry and the Molecular Design Institute, New York University, 100 Washington Square East, New York, NY 10003-6688*

SUPPORTING INFORMATION

Figure S20. Binding of imposter 2e to *R* [0-11] P(+).

Figure S21. Binding of imposter 2e to *R* [0-11] B(+).

Movie 1. Still frame from AFM video movie1_islandformation.avi. Regeneration of DAPSA surface in the presence of a highly supersaturated DAPSA solution (s = 7).

Movie 2. Still frame from AFM video movie2_singledislocation.avi. Spiral growth about a single dislocation on {011} DAPSA in the presence of a supersaturated DAPSA solution (s = 2.5).

Movie 3. Still frame from AFM video movie3_competingdislocations.avi. Spiral growth about two double dislocations of opposite handedness dislocation on the {011} DAPSA in the presence of a supersaturated DAPSA solution (s = 2.5).

Movie 4. Still frame from AFM video movie4_imposter2a.avi. Spiral growth about a Frank-Read source on the {011} DAPSA surface in the presence of a supersaturated DAPSA solution (s = 2.5) and 3 mol% imposter **2a**.

Movie 5. Still frame from AFM video movie5_imposter2e.avi. Spiral growth about a single dislocation on the {011} DAPSA surface in the presence of a supersaturated DAPSA solution (s = 2.5) and 8 mol% imposter **2e**.

Table S1. Crystallographic data and refinement results for the S and R enantiomorphs of DAPSA.

	S Enantiomorph	**R Enantiomorph**
Chemical formula	$C_{14}H_{19}N_5O_4S$	$C_{14}H_{19}N_5O_4S$
Formula weight (g/mol)	353.40	353.40
Temperature (K)	295(2)	295(2)
X-ray wavelength (Å)	0.71073	0.71073
Crystal System	Orthorhombic	Orthorhombic
Space Group	P 21 21 21	P 21 21 21
a (Å)	10.0395(7)	10.0392(6)
b (Å)	10.9015(8)	10.8961(6)
c (Å)	16.0008(12)	15.9916(9)
α (°)	90	90
β (°)	90	90
γ (°)	90	90
Volume ($Å^3$)	1751.2(2)	1749.29(17)
Z	4	4
Density (g/cm^3)	1.340	1.342
Absorption Coefficient (mm^{-1})	0.213	0.213
F(000)	744	744
Crystal size	0.250 x 0.394 x 0.962	0.16 x 0.29 x 0.32
Theta (max)	28.35	28.31
Relfections Collected	20073	20794
Unique Reflections (R_{int})	4374	4354
R(int)	0.0336	0.0597
Goodness-of-fit on F^2	0.885	1.038
R1 [I>2sigma(I)]	0.0337	0.0448
wR2 (all reflections)	0.0908	0.1111
Flack Parameter	0.06(6)	0.02(8)

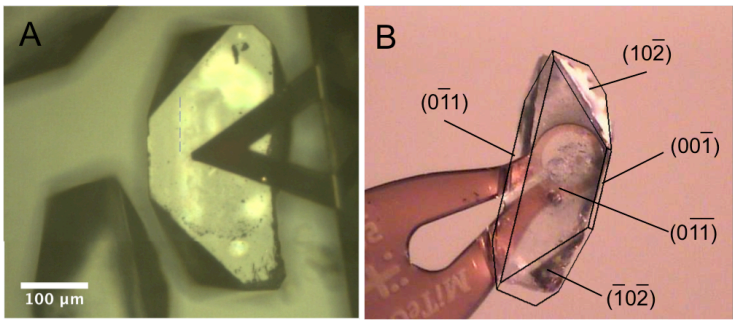

Figure S1. Identification of DAPSA crystal face imaged by AFM. (A) Shape of crystal face typically imaged by AFM. Crystals naturally align with large faces oriented upwards when deposited on the AFM specimen disks. (B) Crystal face indexing by single crystal x-ray diffraction reveals that the {011} faces are consistent with the morphology of the crystal face typically imaged by AFM.

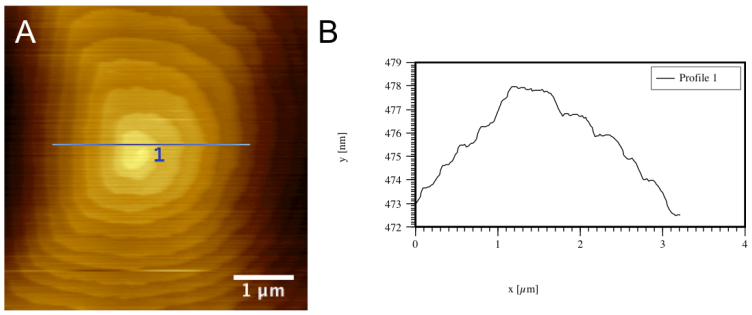

Figure S2. Measurement of {011} DAPSA step heights to confirm the identity of the imaged face. (A) AFM height image of a growth hillock in a supersaturated solution (σ = 2, 0.033 g/L). (B) Profile of the growth hillock in (A) measured along the horizontal line in (A). The average step height was 9.11 ± 1.48 Å (n = 41), which corresponds to the interplanar spacing of the {011} planes.

Protocol for measurement of step velocities

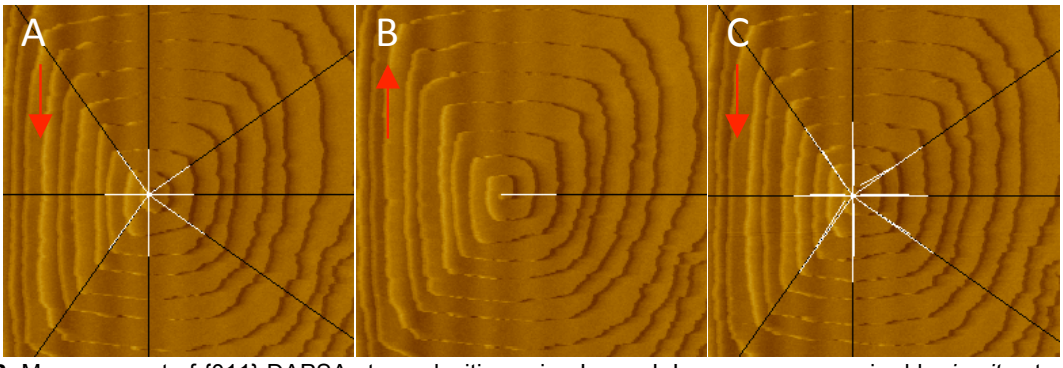

Figure S3. Measurement of {011} DAPSA step velocities using ImageJ. Images were acquired by *in situ* atomic force microscopy as described in the Experimental section. At least 60 images were acquired at a scan rate of 48.8 Hz with a scan size of 5 x 5 µm for a given set of conditions (i.e. solution composition/concentration). Images were converted to .tiff files using Gwyddion, converted to a stack and analyzed using a custom macro in ImageJ (Rasband, W.S., ImageJ, U. S. National Institutes of Health, Bethesda, Maryland, USA, http://imagej.nih.gov/ij/, 1997-2016) to aid in the measurement of step displacement along eight different crystallographic directions.

(A – C) Three consecutive AFM images and corresponding measurement of step displacement for a single step edge along eight different crystallographic directions. The red arrow in each frame indicates the scan direction.

(A) The macro prompts the user to select the dislocation center, and it superimposes black lines on the image along specific crystallographic directions ([100], [2-11], [0-11], [-2-11], [-100], [-11-1], [01-1], [11-1]) to aid measurement of step displacement along these directions. This requires image alignment as illustrated in Figure 3c ([01-1] - left, [0-11] - right, [100] - up, [-100] - down) by alignment of the crystal sample during set up of the AFM or adjustment of the scan angle during image acquisition. The intersections of the black lines with a single step edge along each of the eight crystallographic directions are selected, with white lines indicating where the step edge was measured. The pixel positions (x,y) of the intersection of each step edge with the black guide line is output from the macro.

(B) The opposite scan direction is not used for measurement. The dislocation center is selected and the [0-11] step edge from Frame 1 (A) is selected in Frame 2 to track the same step edge.

(C) For each "down scan" after the first image, the dislocation center is selected and the black lines are superimposed. The white lines indicating the location of the step edge from the previous "down scan" are also superimposed to facilitate tracking of the same step edge along many frames.

The ImageJ macro accounts for drift of the dislocation center by shifting the (x,y) pixel positions of the step edges after the first image by the same amount (in pixels) the dislocation center has shifted from the first image in the stack.

From the output pixel positions, the step velocities along each crystallographic direction for a given step edge were calculated as:

$$v = \frac{\Delta d}{\Delta t}$$

where:

$$\Delta t = t_2 - t_1 = (T_2 - T_1) + \frac{\left|2x_{pix}(y_2 - y_1) + (x_2 - x_1)\right|}{v_{tip}}$$

$$\Delta d = a\sqrt{(x_2 - x_1)^2 + (y_2 - y_1)^2}$$

T1 represents the start time of the image, x_{pix} is the number of pixels per line, and v_{tip} is the velocity of the tip in pixels per second given by

$$v_{tip} = 2(scan\ rate)(scan\ size)$$

and a (nm/pix) is the conversion factor from pixels to spatial dimensions.

At a scan rate of 48.8 Hz and image size of 5 x 5 µm, the following values for these constats were used:

x_{pix} (pixels/line)	258
v_{tip} (pixels/s)	25180.8
a (nm/pix)	19.34
$T_2 - T_1$ (s)	10.49

Table S2. DAPSA molecular imposters and normalized step velocities (V_i/V_o) measured along [01-1] and [0-11] in the presence of a supersaturated solution of DAPSA (σ = 2.5, 0.0385 g/L) upon addition of 5 mol% imposter (based on DAPSA solute). X and Y refer to the substituents on the sulfonamide and 2-amine groups, respectively (Figure 1).

Entry	Compound	Volume difference between imposter and DAPSA ($Å^3$)	X	Volume Difference of X relative to DAPSA ($Å^3$)	Y	Volume Difference of Y relative to DAPSA ($Å^3$)	[01-1] V_i/V_o	[0-11] V_i/V_o
1	**DAPSA**	-	NH_2	-	H	-	1	1
2	**1a**	8	CH_3	8	H	0	0.45 ± 0.11	0.71 ± 0.08
3	**1b**	44	CH_2CH_3	44	H	0	0.45 ± 0.20	0.96 ± 0.23
4	**1c**	94	$NHCH_2CH_3$	95	H	0	0	0
5	**1d**	97	$CH_2CH_2CH_3$	97	H	0	0.04 ± 0.03	0.21 ± 0.08
6	**2a**	58	CH_3	8	CH_3	49	0	0
7	**2b**	114	CH_3	8	CH_2CH_3	106	0.87 ± 0.10	0.56 ± 0.06
8	**2c**	156	CH_3	8	$CH_2(CH_2)_2$	148	1.10 ± 0.10	1.18 ± 0.14
9	**2d**	200	CH_3	8	$CH_2CH_2(CH_2)_2$	192	1.23 ± 0.07	0.93 ± 0.11
10	**2e**	240	CH_3	8	CHC_6H_5	232	1.28 ± 0.17	0.69 ± 0.07
11	**2f**	143	CH_3	8	CH_2 CH_2OH	134	0.85 ± 0.06	0.80 ± 0.05
12	**2g**	199	CH_3	8	CH_2 CH_2OCH_3	191	0.90 ± 0.04	0.85 ± 0.06
13	**3a**	-97	NH_2*	-97	H	0	0.35 ± 0.06	0.92 ± 0.05
14	**3b**	-62	I *	-62	H	0	0.27 ± 0.06	0.76 ± 0.02
15	**3c**	-59	C≡C *	-60	H	0	0.05 ± 0.04	0.57 ± 0.12
16	**4a**†	7	NH_2	0	H	0	0.68 ± 0.13	0.81 ± 0.08
17	**5a**†	-207	H	-207	H	0	0.66 ± 0.10	1.13 ± 0.09
18	**5b**†	-275	H	-275	H	0	0.72 ± 0.05	0.73 ± 0.13
19	**5c**	-129	H	-129	H	0	0.27 ± 0.06	1.06 ± 0.06
20	**Trimetho-prim**†	281	-	-	-	-	0.91 ± 0.07	0.95 ± 0.07
21	**Sulfanil-amide**†	-112	-	-	-	-	0.79 ± 0.04	1.06 ± 0.07
22	**Sulfa-diazine**†	-466	-	-	-	-	1.02 ± 0.08	1.10 ± 0.09
23	**Dofe-tilide**†	-287	-	-	-	-	0.88 ± 0.05	0.78 ± 0.06

* the entire sulfonamide moiety of DAPSA is replaced.

† functional groups of the DAPSA backbone other than X and Y are also modified

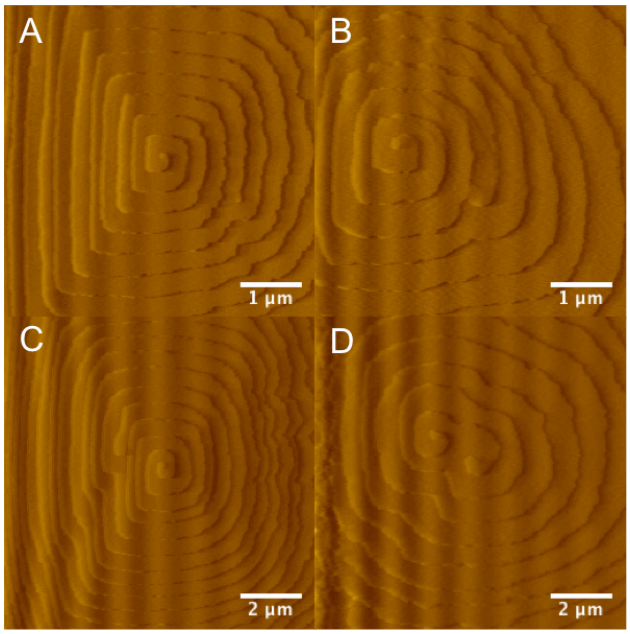

Figure S4. In situ AFM images of hillocks on {011} DAPSA in the presence of a supersaturated solution of DAPSA (σ = 2.5, 0.0385 g/L) with no imposter (A) and in the presence of 3 mol% (B), 5 mol% (C) and 8 mol% (D) trimethoprim. All images are oriented with crystallographic directions depicted in Figure 3c.

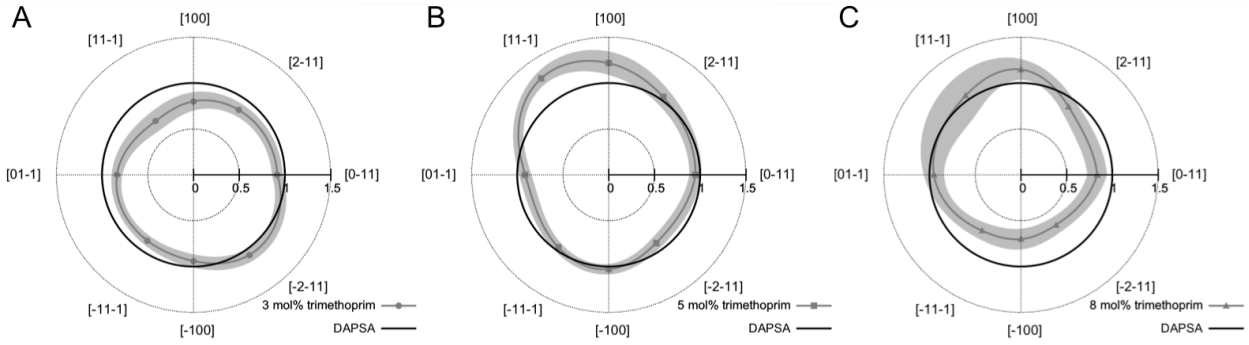

Figure S5. Normalized step velocities (V_i/V_o) measured along specific crystallographic directions in the presence of a supersaturated solution of DAPSA (σ = 2.5, 0.0385 g/L) upon addition of 3 mol% (A), 5 mol% (B), and 8 mol% (C) trimethoprim. The circle at r = 1 represents the self-normalized V_o for DAPSA along every direction in a supersaturated solution of DAPSA without imposter (σ = 2.5, 0.0385 g/L). V_i is the step velocity measured in the presence of a supersaturated solution of DAPSA (σ = 2.5, 0.0385 g/L) containing the molecular imposter at the indicated concentration.

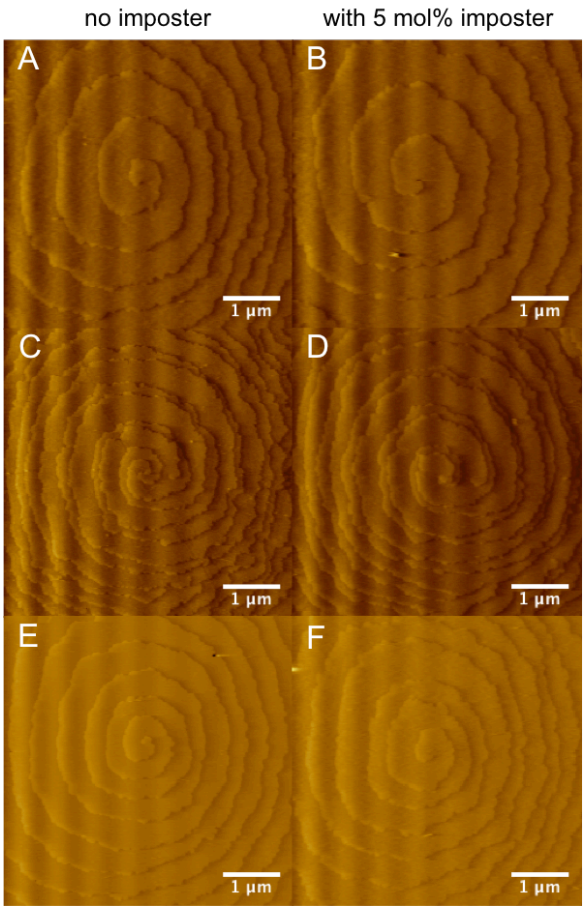

Figure S6. In situ AFM images of hillocks on {011} DAPSA in the presence of a supersaturated solution of DAPSA (σ = 2.5, 0.0385 g/L) with no imposter (left panel) and in the presence of 5 mol% of imposter (right panel). (A,B) Before and after addition of sulfanilamide, (C,D) before and after addition of sulfadiazine, and (E,F) before and after addition of dofetilide. All FDA-approved drugs cause no noticeable change in hillock morphology. All images are oriented with crystallographic directions depicted in Figure 3c.

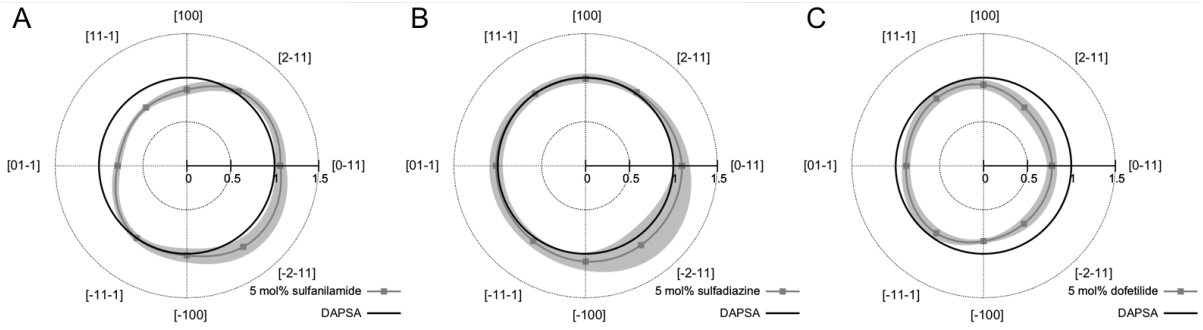

Figure S7. Normalized step velocities (V_i/V_o) measured along specific crystallographic directions in the presence of a supersaturated solution of DAPSA (σ = 2.5, 0.0385 g/L) upon addition of 5 mol% sulfanilamide (A), sulfadiazine (B), and dofetilide (C). The circle at r = 1 represents the self-normalized V_o for DAPSA along every direction in a supersaturated solution of DAPSA without imposter (σ = 2.5, 0.0385 g/L). V_i is the step velocity measured in the presence of a supersaturated solution of DAPSA (σ = 2.5, 0.0385 g/L) containing the molecular imposter at the indicated concentration.

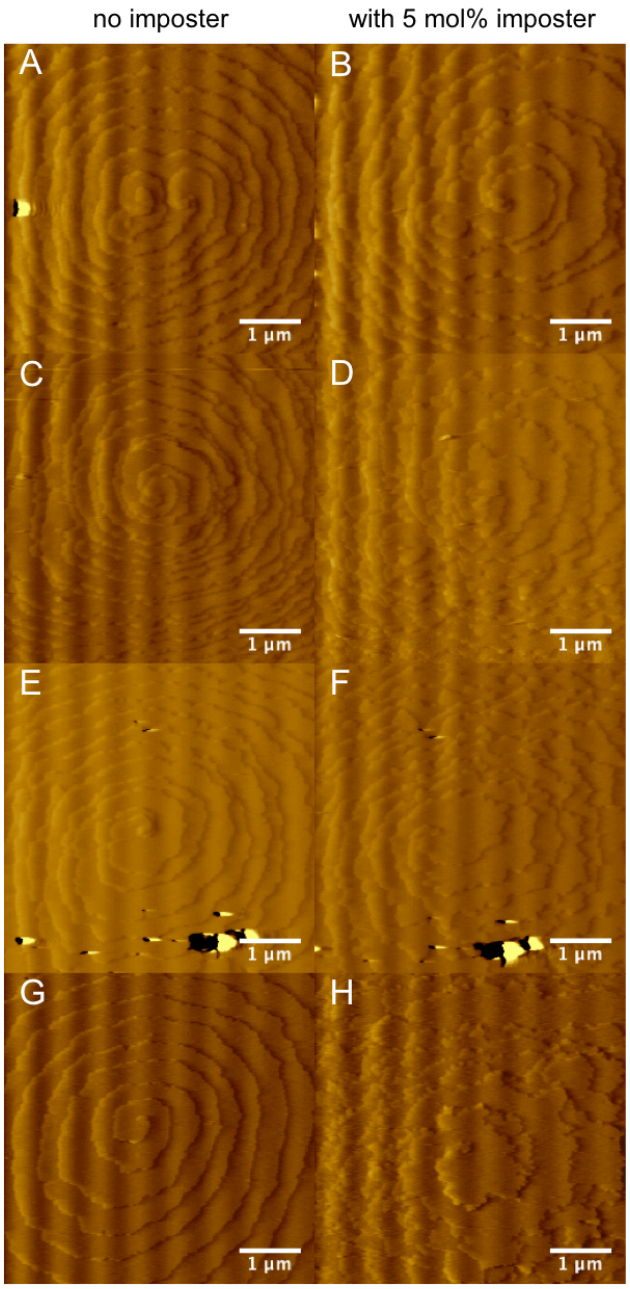

Figure S8. In situ AFM images of hillocks on {011} DAPSA in the presence of a supersaturated solution of DAPSA (σ = 2.5, 0.0385 g/L) with no imposter (left panel) and in the presence of 5 mol% (right panel) of **1a** (B), **1b** (D), **1c** (F), and **1d** (H). All images are oriented with crystallographic directions depicted in Figure 3c. *Growth ceased completely upon addition of **1c** and growth was negligible upon addition of **1d**.*

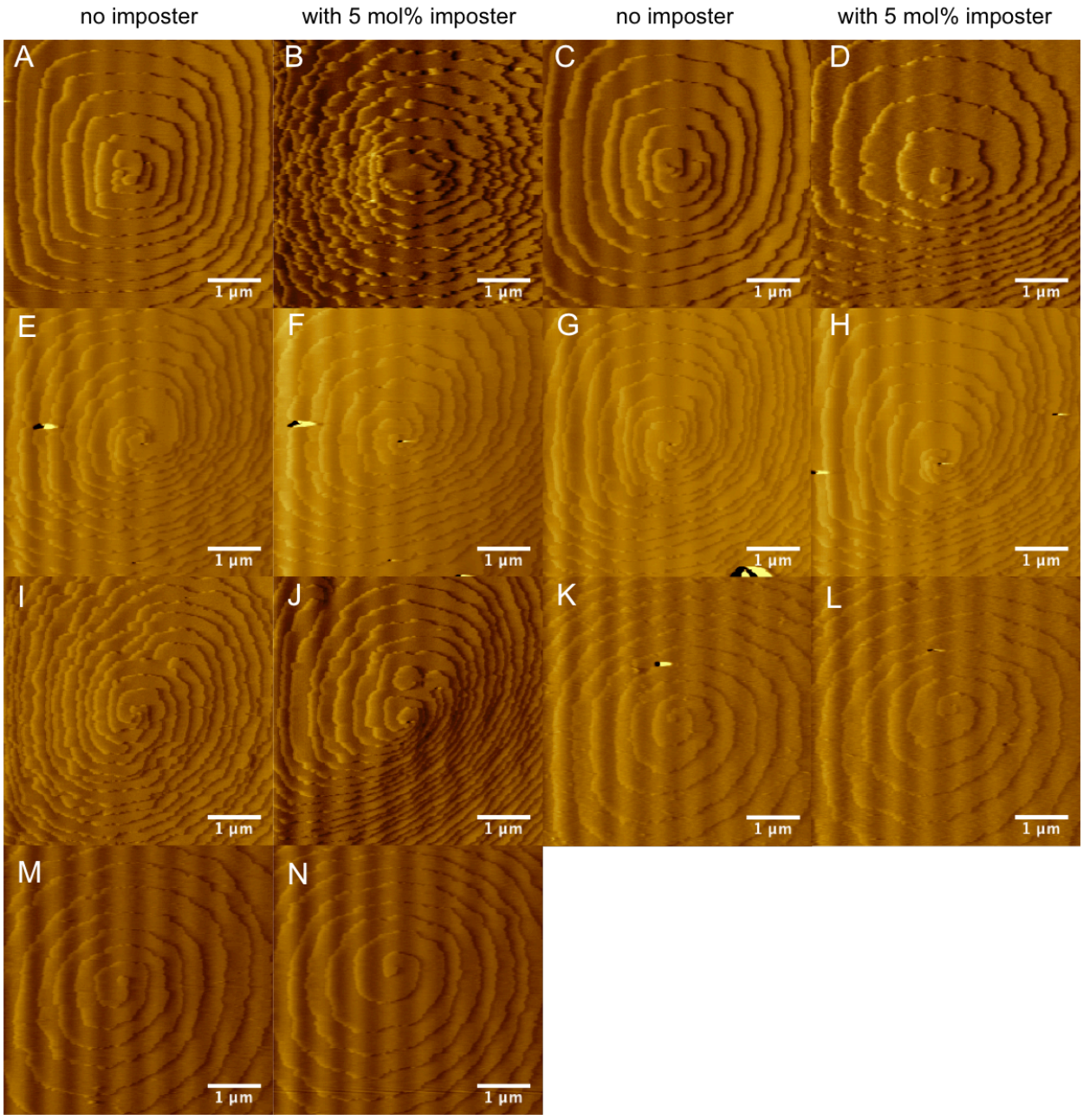

Figure S9. In situ AFM images of hillocks on {011} DAPSA in the presence of a supersaturated solution of DAPSA (σ = 2.5, 0.0385 g/L) with no imposter and in the presence of 5 mol% of Group 2 imposters. (A,B) Before and after addition of **2a**, (C,D) before and after addition of **2b**, (E,F) before and after addition of **2c**, (G,H) before and after addition of **2d**, (I,J) before and after addition of **2e**, (K,L) before and after addition of **2f**, and (M,N) before and after addition of **2g**. Only **2a**, **2b**, and **2e** produce noticeable changes in hillock morphology. All images are oriented with crystallographic directions depicted in Figure 3c.

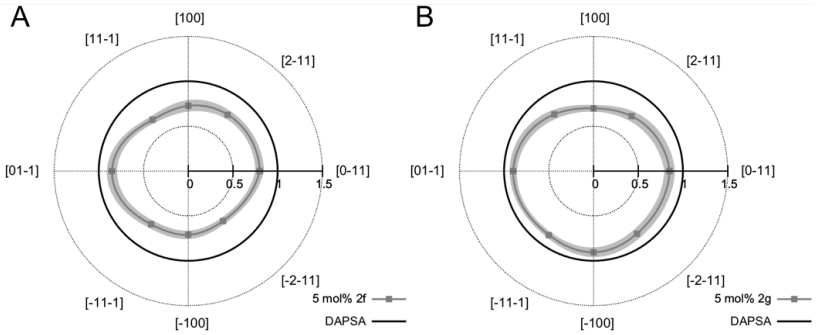

Figure S10. Normalized step velocities (V_i/V_o) measured along specific crystallographic directions in the presence of a supersaturated solution of DAPSA (σ = 2.5, 0.0385 g/L) upon addition of 5 mol% **2f** (A) and **2g** (B). The circle at r = 1 represents the self-normalized V_o for DAPSA along every direction in a supersaturated solution of DAPSA without imposter (σ = 2.5, 0.0385 g/L). V_i is the step velocity measured in the presence of a supersaturated solution of DAPSA (σ = 2.5, 0.0385 g/L) containing the molecular imposter at the indicated concentration.

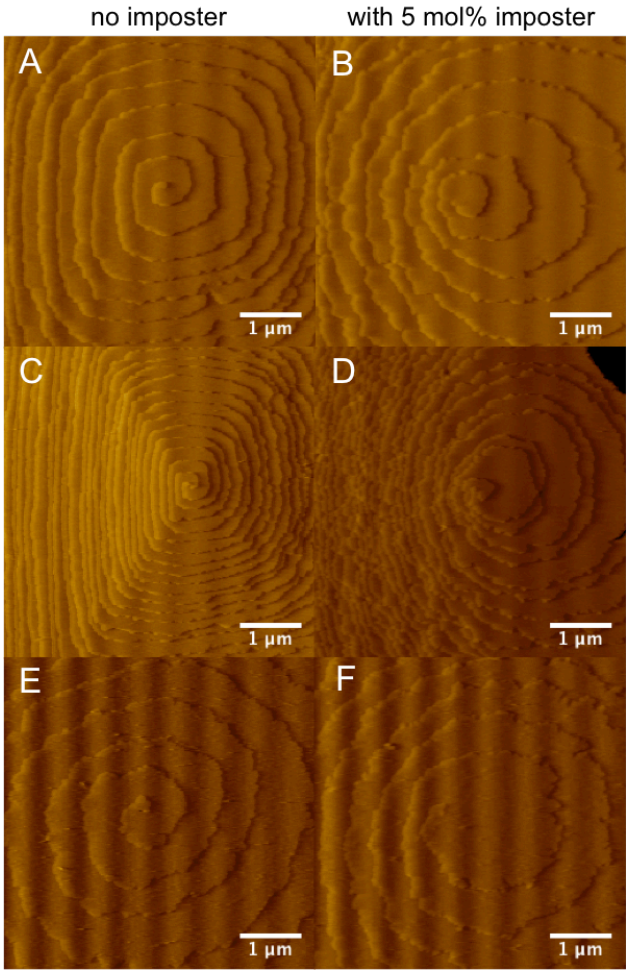

Figure S11. In situ AFM images of hillocks on {011} DAPSA in the presence of a supersaturated solution of DAPSA (σ = 2.5, 0.0385 g/L) with no imposter (left panel) and in the presence of 5 mol% (right panel) of **3a** (B), **3b** (D), and **3c** (F). All images are oriented with crystallographic directions depicted in Figure 3c.

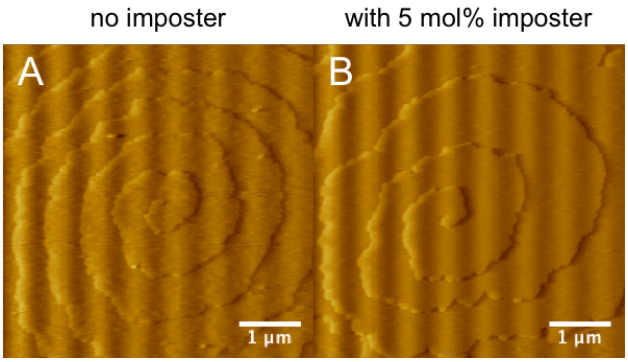

Figure S12. In situ AFM images of hillocks on {011} DAPSA in the presence of a supersaturated solution of DAPSA (σ = 2.5, 0.0385 g/L) with no imposter (A) and in the presence of 5 mol% of **4a** (B). All images are oriented with crystallographic directions depicted in Figure 3c.

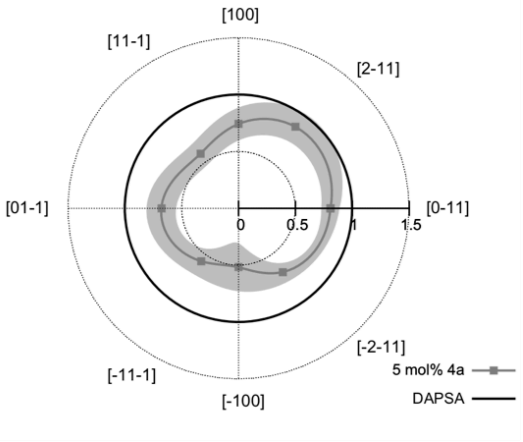

Figure S13. Normalized step velocities (V_i/V_o) measured along specific crystallographic directions in the presence of a supersaturated solution of DAPSA (σ = 2.5, 0.0385 g/L) upon addition of 5 mol% **4a**. The circle at r = 1 represents the self-normalized V_o for DAPSA along every direction in a supersaturated solution of DAPSA without imposter (σ = 2.5, 0.0385 g/L). V_i is the step velocity measured in the presence of a supersaturated solution of DAPSA (σ = 2.5, 0.0385 g/L) containing the molecular imposter at the indicated concentration.

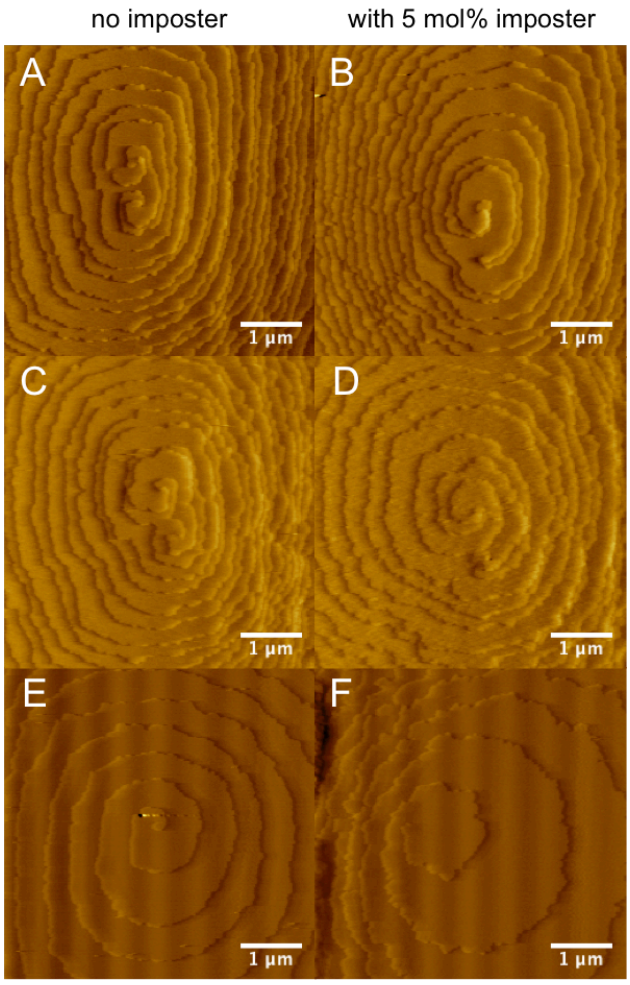

Figure S14. In situ AFM images of hillocks on {011} DAPSA in the presence of a supersaturated solution of DAPSA (σ = 2.5, 0.0385 g/L) with no imposter (left panel) and in the presence of 5 mol% (right panel) of **5a** (B), **5b** (D), and **5c** (F). All images are oriented with crystallographic directions depicted in Figure 3c.

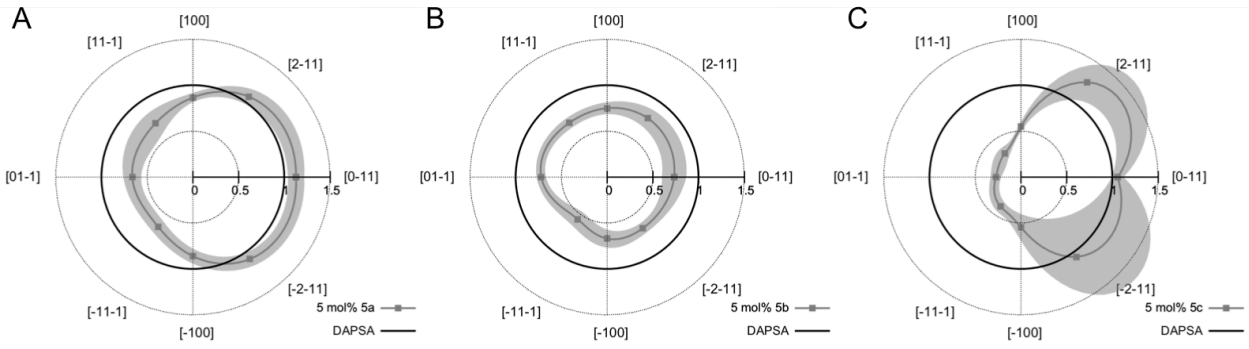

Figure S15. Normalized step velocities (V_i/V_o) measured along specific crystallographic directions in the presence of a supersaturated solution of DAPSA (σ = 2.5, 0.0385 g/L) upon addition of 5 mol% **5a** (A), **5b** (B), and **5c** (C). The circle at r = 1 represents the self-normalized V_o for DAPSA along every direction in a supersaturated solution of DAPSA without imposter (σ = 2.5, 0.0385 g/L). V_i is the step velocity measured in the presence of a supersaturated solution of DAPSA (σ = 2.5, 0.0385 g/L) containing the molecular imposter at the indicated concentration.

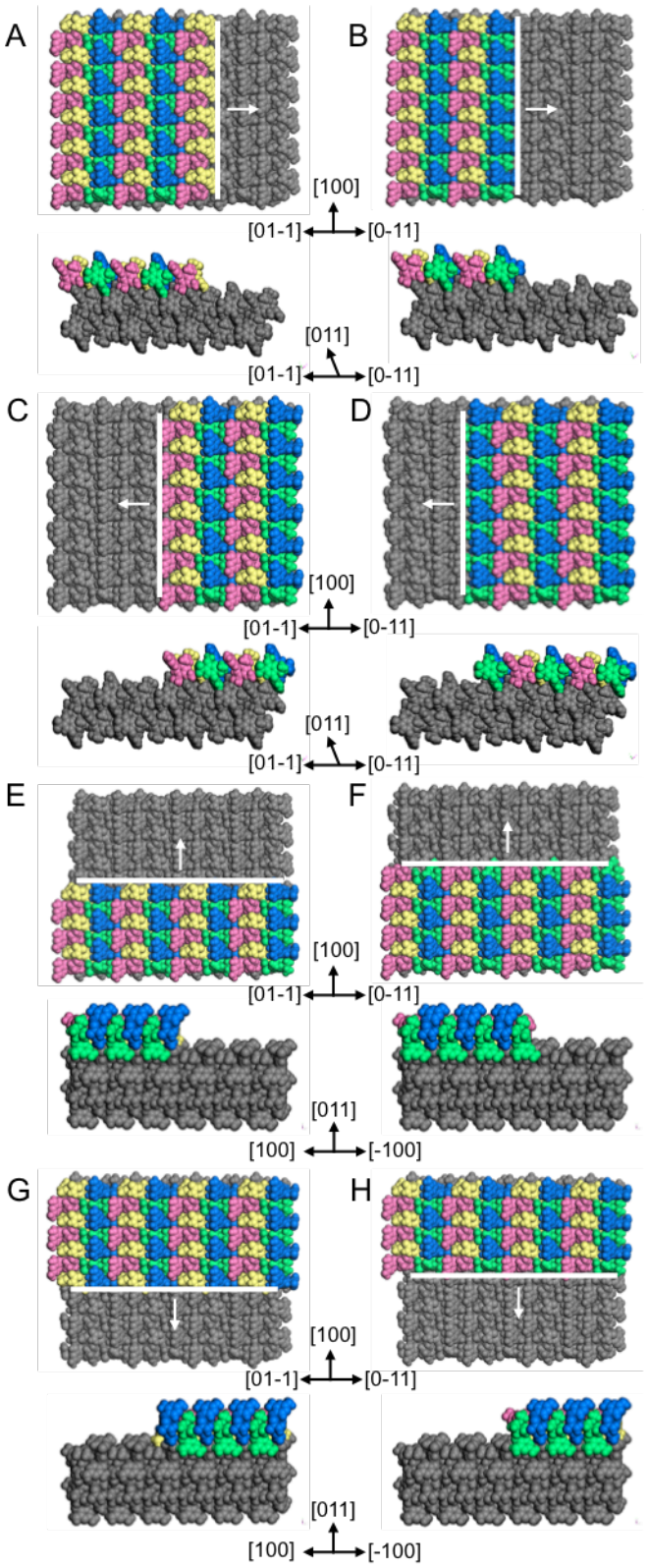

Figure S16. Step edges perpendicular to the [0-11] (A-B), [01-1] (C-D), [100] (E-F), and [-100] (G-H) directions on the (011) DAPSA surface. Color scheme corresponds to that used for the four asymmetric units in Figure 2 (P = pink, Y = yellow, B = blue, G = green).

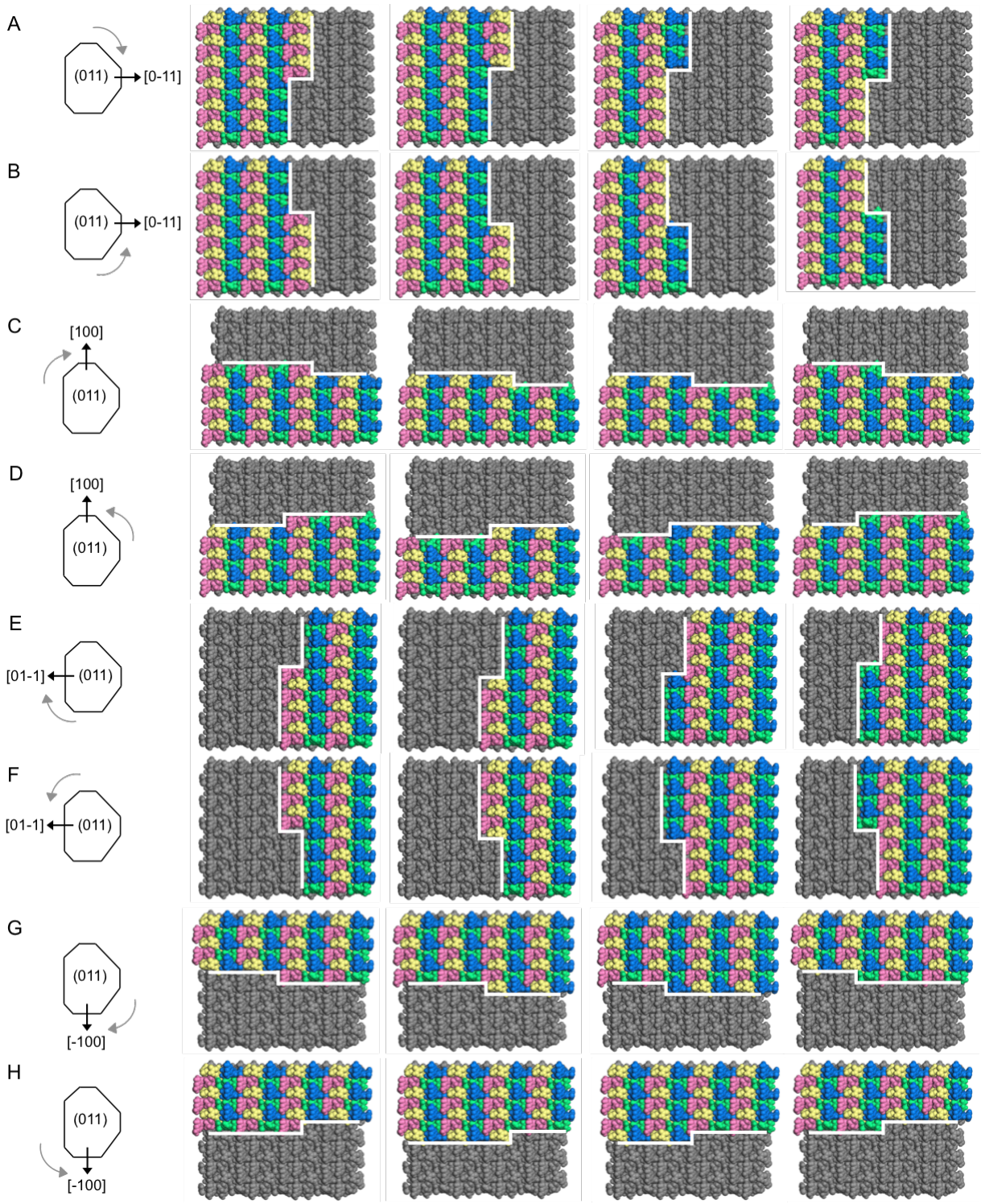

Figure S17. "Clockwise" (A,C,E,G) and "counter-clockwise" (B,D,F,H) kink sites on the step edge propagating along the [0-11] (A-B), [100] (C-D), [01-1] (E-F), and [-100] (G-H) directions on the (011) surface. Kink sites are characterized by the orientation of the molecule binding at the kink: pink (first panel), yellow (second panel), blue (third panel) and green (fourth panel).

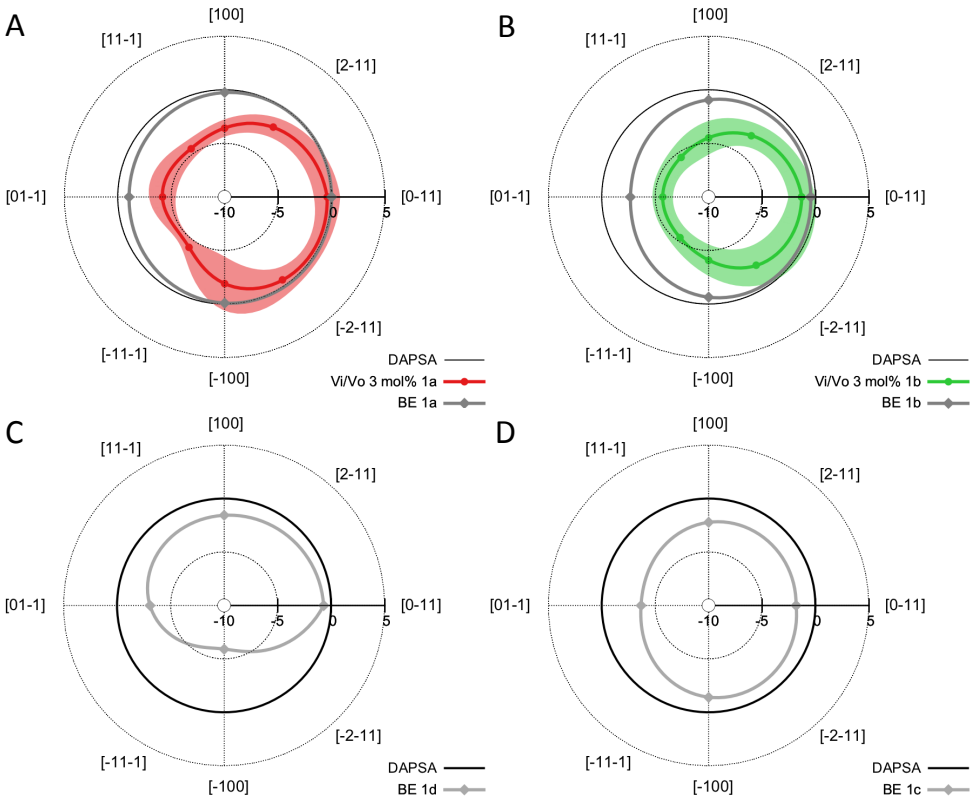

Figure S18. Wulff-like plots of the lowest relative imposter-kink binding energy (kcal/mol) along [100], [01-1], [-100], and [0-11] of the DAPSA R (dark gray) enantiomorph for imposters (A) **1a**, (B) **1b**, (C) **1c**, and (D) **1d**. For each imposter, the lowest imposter-kink binding energy along [100], [01-1], [-100], and [0-11] was selected and a curve was obtained by interpolation.

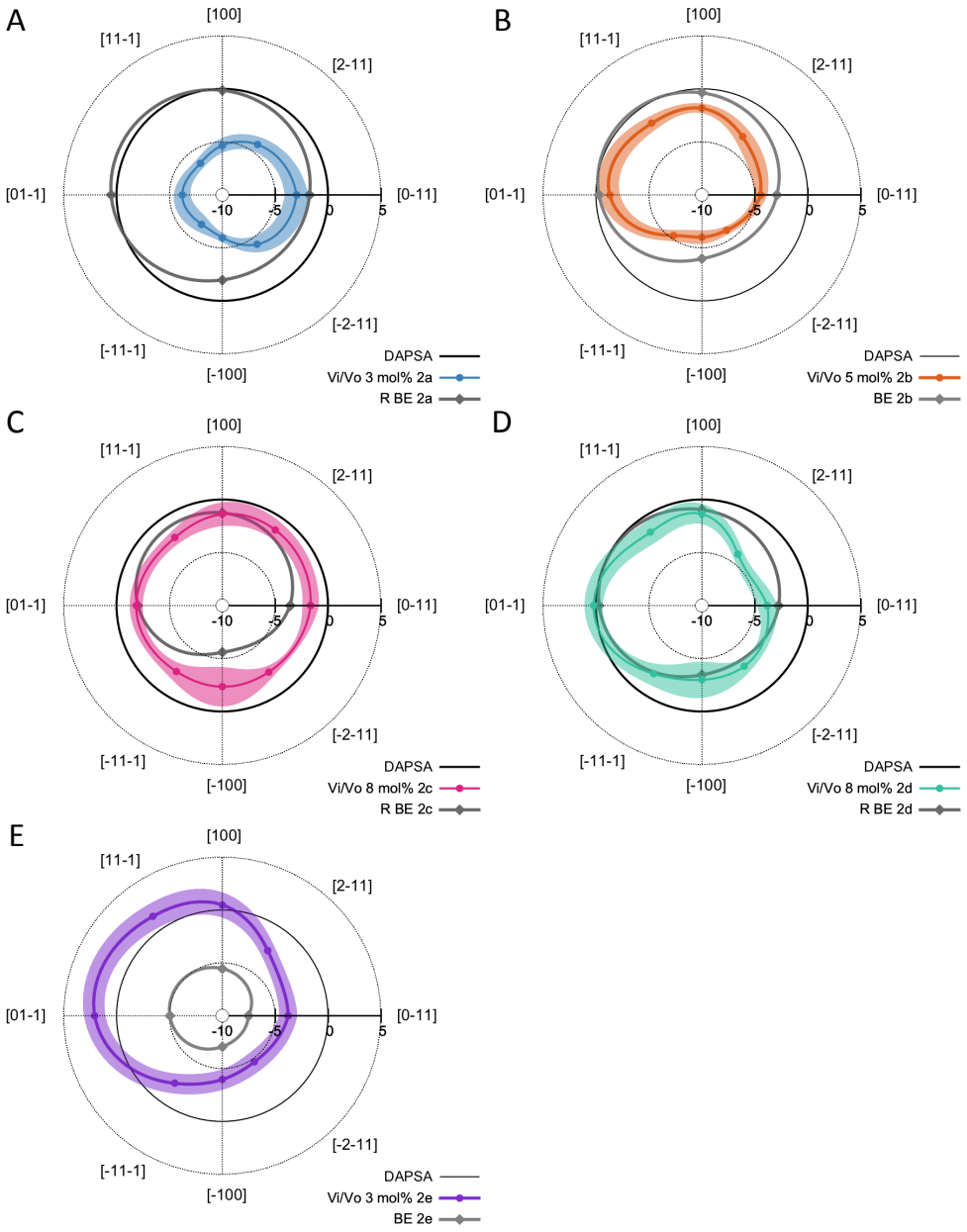

Figure S19. Wulff-like plots of the lowest relative imposter-kink binding energy (kcal/mol) along [100], [01-1], [-100], and [0-11] of the DAPSA R (dark gray) enantiomorph for imposters (A) **2a**, (B) **2b**, (C) **2c**, (D) **2d**, and (E) **2e**. For each imposter, the lowest imposter-kink binding energy along [100], [01-1], [-100], and [0-11] was selected and a curve was obtained by interpolation.

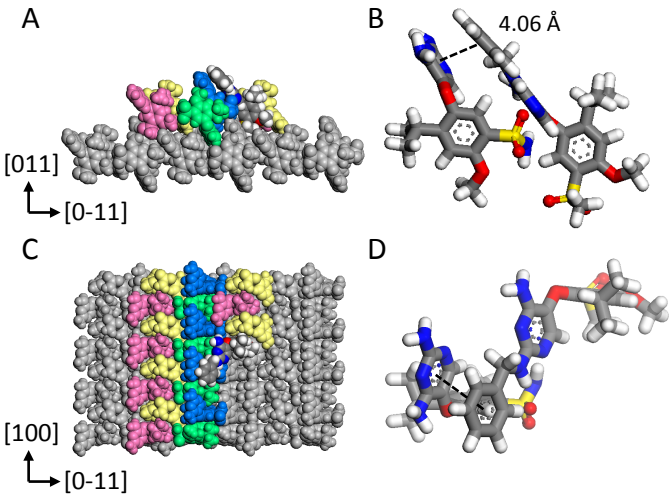

Figure S20. Binding of imposter **2e** to *R* [0-11] P(+). The distance between the centroid of the phenyl group of imposter **2e** and the centroid of the diaminopyrimidine moiety of DAPSA molecule comprising the step edge suggests π-π stacking interactions that facilitate the binding of this imposter at the DAPSA surface.

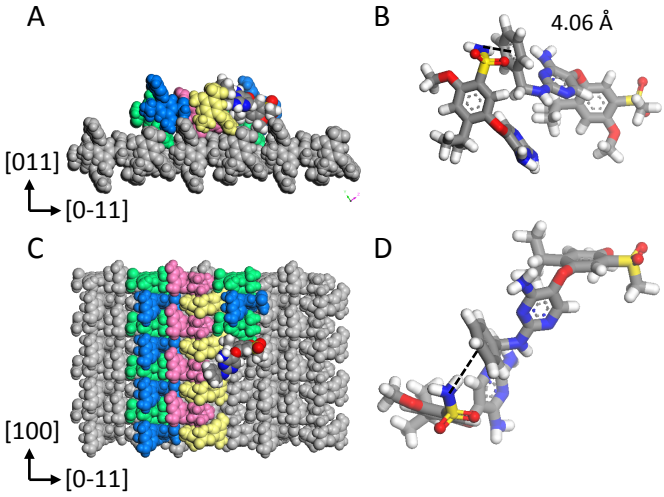

Figure S21. Binding of imposter **2e** to *R* [0-11] B(+). The distance between the centroid of the phenyl group of imposter **2e** and the nitrogen of the sulfonamide moiety on a DAPSA molecule comprising the step edge suggests favorable interactions that facilitate the binding of this imposter at the DAPSA surface.

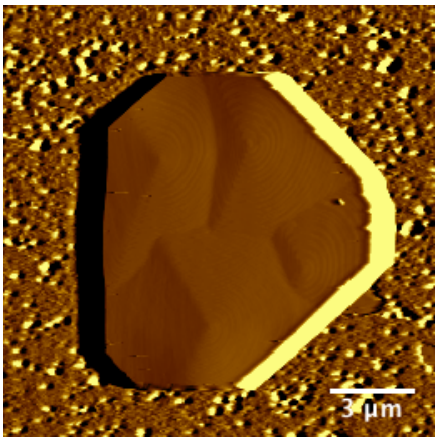

Movie 1. Still frame from AFM video movie1_islandformation.avi depicting regeneration of the {011} DAPSA surface at a high supersaturation. Consecutive *in situ* AFM images of the {011} DAPSA surface in a highly supersaturated DAPSA solution (σ = 7, 0.0880 g/L) reveal hillocks on the {011} growth island, the shape of which reflects the shape of the {011} DAPSA crystal face (Figure 3).

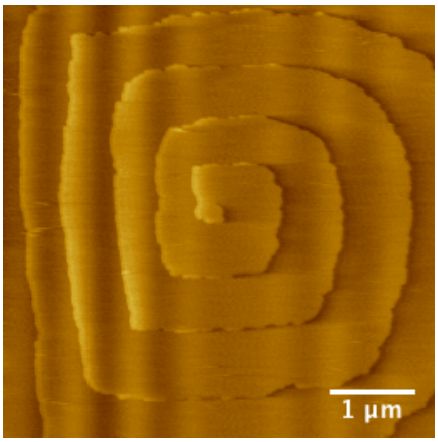

Movie 2. Still frame from AFM video movie2_singledislocation.avi depicting spiral growth about a single dislocation on the {011} DAPSA surface in the presence of a supersaturated DAPSA solution (σ = 2.5, 0.0385 g/L).

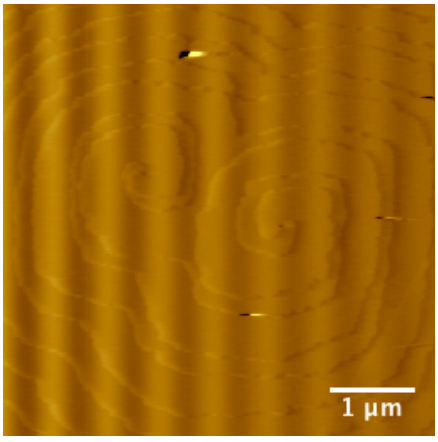

Movie 3. Still frame from AFM video movie 3_competingdislocations.avi depicting spiral growth about two double dislocations of opposite handedness on the {011} DAPSA surface in the presence of a supersaturated DAPSA solution (σ = 2.5, 0.0385 g/L).

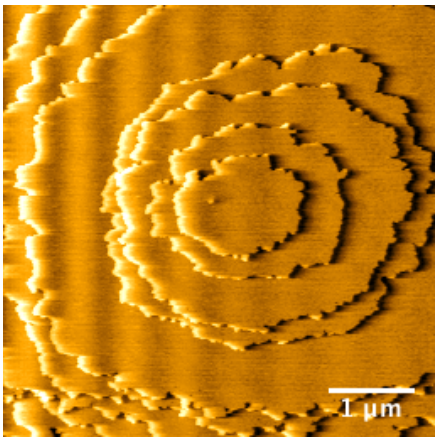

Movie 4. Still frame from AFM video movie4_imposter2a.avi depicting spiral growth about a Frank-Read dislocation source on the {011} DAPSA surface in the presence of a supersaturated DAPSA solution (σ = 2.5, 0.0385 g/L) and 3 mol% imposter **2a**.

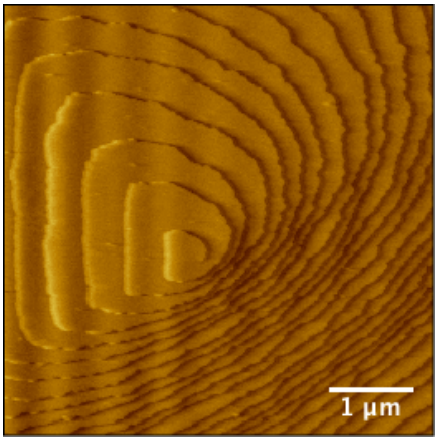

Movie 5. Still frame from AFM video movie5_imposter2e.avi depicting spiral growth about a single dislocation on the {011} DAPSA surface in the presence of a supersaturated DAPSA solution (σ = 2.5, 0.0385 g/L) and 8 mol% imposter **2e**.